

## ARTICLE

# Combining recombinase polymerase amplification and DNA-templated reaction for SARS-CoV-2 sensing with dual fluorescence and lateral flow assay output

Lluc Farrera-Soler | Arthur Gonse | Ki Tae Kim | Sofia Barluenga |  
Nicolas Winssinger 

Department of Organic Chemistry, NCCR  
Chemical Biology, Faculty of Science,  
University of Geneva, Geneva, Switzerland

**Correspondence**

Nicolas Winssinger, Department of Organic  
Chemistry, NCCR Chemical Biology, Faculty of  
Science, University of Geneva, 30 quai Ernest  
Ansermet, 1211 Geneva, Switzerland.  
Email: nicolas.winssinger@unige.ch

**Funding information**

Département d'instruction public (DIP) du  
canton de Genève; University of Geneva

**Abstract**

The early phase of the severe acute respiratory syndrome coronavirus 2 (SARS-CoV-2) pandemic was exacerbated by a diagnostic challenge of unprecedented magnitude. In the absence of effective therapeutics or vaccines, breaking the chain of transmission through early disease detection and patient isolation was the only means to control the growing pandemic. While polymerase chain reaction (PCR)-based methods and rapid-antigen tests rose to the occasion, the analytical challenge of rapid and sequence-specific nucleic acid-sensing at a point-of-care or home setting stimulated intense developments. Herein we report a method that combines recombinase polymerase amplification and a DNA-templated reaction to achieve a dual readout with either fluorescence (microtiter plate) or naked eye (lateral flow assay: LFA) detection. The nucleic acid templated reaction is based on an  $S_NAr$  that simultaneously transfers biotin from one Peptide Nucleic Acid (PNA) strand to another PNA strand, enabling LFA detection while uncaging a coumarin for fluorescence readout. This methodology has been applied to the detection of a DNA or RNA sequence uniquely attributed to the SARS-CoV-2.

**KEYWORDS**

DNA templated reaction, lateral flow assay, nucleic acid sensing, PNA, RPA

## 1 | INTRODUCTION

Historically, respiratory viral detection has been achieved by analyzing the presence of viral genomes from nasal or throat swabs.<sup>[1]</sup> Nucleic acid amplification tests (NAAT) are based on an oligonucleotide amplification step coupled to a detection method. Quantitative real-time PCR (qPCR) is the gold standard and most frequently used strategy. It consists of repetitive cycles of heat/cool to melt, anneal and perform primer extension by polymerase, thus affording an amplification that is exponentially correlated to the number of cycles (typically 25-

35).<sup>[2,3]</sup> The detection step is generally performed by fluorescence readout<sup>[4]</sup> using either non-specific fluorescent dye that intercalates double-stranded DNA (dsDNA) (ethidium bromide<sup>[5]</sup> or SYBR Gold)<sup>[6]</sup> or sequence-specific probes with fluorescent reporters.<sup>[7,8]</sup> The unprecedented scale and propagation speed of the SARS-CoV-2 pandemic resulted in a demand for diagnostic tests that far exceeded specialized facilities' capacity and, turn-around which often exceeded 24 h. In the absence of effective therapeutics or vaccines, breaking the chain of transmission through early disease detection and patient isolation is the only means to control an epidemic. Fast and readily

This is an open access article under the terms of the Creative Commons Attribution-NonCommercial License, which permits use, distribution and reproduction in any medium, provided the original work is properly cited and is not used for commercial purposes.

© 2022 The Authors. *Biopolymers* published by Wiley Periodicals LLC.

available testing is critical to curtailing broader community spreading. The ideal case would be to have a simple and inexpensive technology compatible with self-testing. The World Health Organization (WHO) emphasized the importance of developing highly sensitive viral tests that could be easily performed by non-professional personnel.<sup>[9,10]</sup> While this issue was largely resolved in the spring of 2021 with rapid antigen detection test (RADT),<sup>[11,12]</sup> which are based on the detection of viral proteins using antibodies in a lateral flow assay (LFA) format, the SARS-CoV-2 crisis propelled a quest for user-friendly nucleic acid-sensing technologies that can be performed outside of specialized laboratory settings. This demand can be extrapolated to the emergence of new SARS-CoV-2 strains and other pathogens. A major limitation of a qPCR assay is the need for a specialized instrument for thermocycling and fluorescence detection. For the amplification, alternatives that do not require thermocycling are well established, namely loop-mediated isothermal amplification (LAMP)<sup>[13–15]</sup> (Figure S1) or recombinase polymerase amplification (RPA)<sup>[16–18]</sup> (Figure S1). The readout can be a simple amplicon quantification but preferably incorporates a sequence specificity component to eliminate false positives arising from amplification of mishybridized primers. Isothermal amplification can be more promiscuous than qPCR, increasing the relevance of this latter point. The sequence specificity can be achieved by targeting the region between the primers with hybridization probes, CRISPR-Cas with guide RNA, or by nucleic acid templated reactions (Figure S1). For the detection, while a fluorescent readout provides sensitive real-time measurements, naked-eye detection methods are more desirable for point-of-care diagnostics and can be performed with colorimetric changes, LFA, or using inexpensive electronics. Different combinations of isothermal amplifications<sup>[19]</sup> and readout with naked-eye detection have been reported for SARS-CoV-2, including LAMP with a colorimetric or fluorescent detection,<sup>[20–28]</sup> RPA with hybridization probes,<sup>[29–34]</sup> LAMP with CRISPR/Cas12,<sup>[35]</sup> RPA with CRISPR/Cas12a,<sup>[36,37]</sup> RPA with CRISPR/Cas9a detection<sup>[38]</sup> and RPA with templated XNAzyme.<sup>[39]</sup> In terms of amplification, RPA stands out for being performed at human body temperature (37 °C) and, therefore, could be performed without any external instrument by just using the human corporal heat.<sup>[40]</sup> Nucleic acid detection by templated chemical reactions<sup>[41–45]</sup> has been shown to yield high sequence fidelity and be highly robust, operating within highly complex biological samples. While the template can act catalytically, affording some signal amplification ( $10^2$ – $10^4$ ), the level of amplification is not sufficient for the detection threshold required for SARS-CoV-2 infection screen (several copies/ $\mu$ L).<sup>[46]</sup> We reasoned that coupling RPA with a templated reaction might yield a robust solution, providing high amplification at isothermal conditions with high-sequence specificity from the templated reaction. For detection, LFA remains a method of choice for its quick, easily adaptable, and user-friendly characteristics.<sup>[47,48]</sup> The simplicity of the assay and the naked eye readout makes it amenable to end-users without specialized equipment. However, it only provides an end-point measurement which can be cumbersome in the assay optimization phase, and it is laborious to multiplex. We reasoned that ideally, the assay should have a dual readout with a fluorescence signal that can be monitored in real-time and easily multiplexed in a plate reader in a lab, as well as an LFA readout for home / field use. Inspired

by the work of Abe and co-workers using a nucleophilic aromatic substitution ( $S_NAr$ ) reaction, involving a thiol nucleophile and a nitroaryl sulfonyl-caged aminocoumarin,<sup>[49]</sup> we asked if the nitroaryl could be further functionalized with biotin to achieve a dual-read out (Figure 1). We selected PNA<sup>[50]</sup> for the probes based on their high sequence fidelity of hybridization, in particular using gamma-modified PNA,<sup>[51]</sup> coupled to their metabolic stability and overall robustness.<sup>[52]</sup> Notably, high-single nucleotide polymorphism (SNP) resolution had been demonstrated with PNA-based templated reaction in conjunction with PCR.<sup>[53,54]</sup> LFA detection had already been demonstrated with PNA-templated reactions for the detection of miRNA<sup>[55,56]</sup> but the reported technology used a ligation reaction affording a product with higher affinity to the template, resulting in product inhibition. Herein we report the detection of single-stranded DNA (ssDNA) via single-strand RPA amplification (RPA amplification + exonuclease degradation) coupled to the proposed DNA-templated nucleophilic aromatic substitution ( $S_NAr$ ) reaction, which transfers the biotin-functionalized aryl moiety from one PNA to the other without a ligation (Figure 1). The use of an LFA detectable label (Fluorescein Isothiocyanate: FITC) on the latter strand enables the detection of the reaction output by LFA. The  $S_NAr$  reaction also unmasks the fluorescence of the aminocoumarin, enabling real-time monitoring of the reaction progress. Finally, we demonstrate that the procedure can be combined with a reverse transcriptase (RT) to analyze RNA.

## 2 | MATERIALS AND METHODS

### 2.1 | Synthesis of PNA probes

PNA probes were synthesized by Solid Phase Peptide Synthesis (SPPS) on an Intavis AG Multiprep RS instrument.<sup>[57,58]</sup> Briefly, to 5.0 mg of Nova PEG Rink amide resin (0.44 mmol/g, NovaBiochem), iterative cycles of amide coupling (5.0 equivalents monomer, 4.0 equivalents 1-[Bis(dimethylamino)methylene]-1H-1,2,3-triazolo[4,5-b]pyridinium 3-oxide hexafluorophosphate (HATU), 5.0 equivalents N, N-Diisopropylethylamine (DIPEA) and 7.5 equivalents 2,6-lutidine), capping of the resin, and deprotection were done. Serine modified PNA monomers at the  $\gamma$  position (A\*, C\*, G\*, T\*) were intercalated with unmodified achiral monomers (A, C, G, T). These Serine modifications at the  $\gamma$  position confer helicity to the PNA, enhancing its affinity and specificity while increasing its solubility. Finally, PNA probes were deprotected and cleaved from the resin with a mixture of TFA and scavengers (440  $\mu$ L of TFA + 25 mg phenol + 25  $\mu$ L water + 10  $\mu$ L triisopropylsilane) for 2 h, precipitated in cold ether and purified by High-performance liquid chromatography (HPLC). The purity was assessed either by Matrix-assisted laser desorption/ionization (MALDI) or Liquid chromatography-mass spectrometry (LC-MS).

For PNA probes bearing a nucleophile and without fluorescein (HX-PNA), the synthesis was done by first coupling Fmoc-DAP(Mtt)-OH on the C' terminus followed by Mtt deprotection of the side chain, eight couplings of PNA monomer, acetylation of the free  $NH_2$  on the last PNA monomer, Fmoc deprotection of the L-2,3-diamino propionic acid (DAP), and finally coupling a polyethylene glycol (PEG)

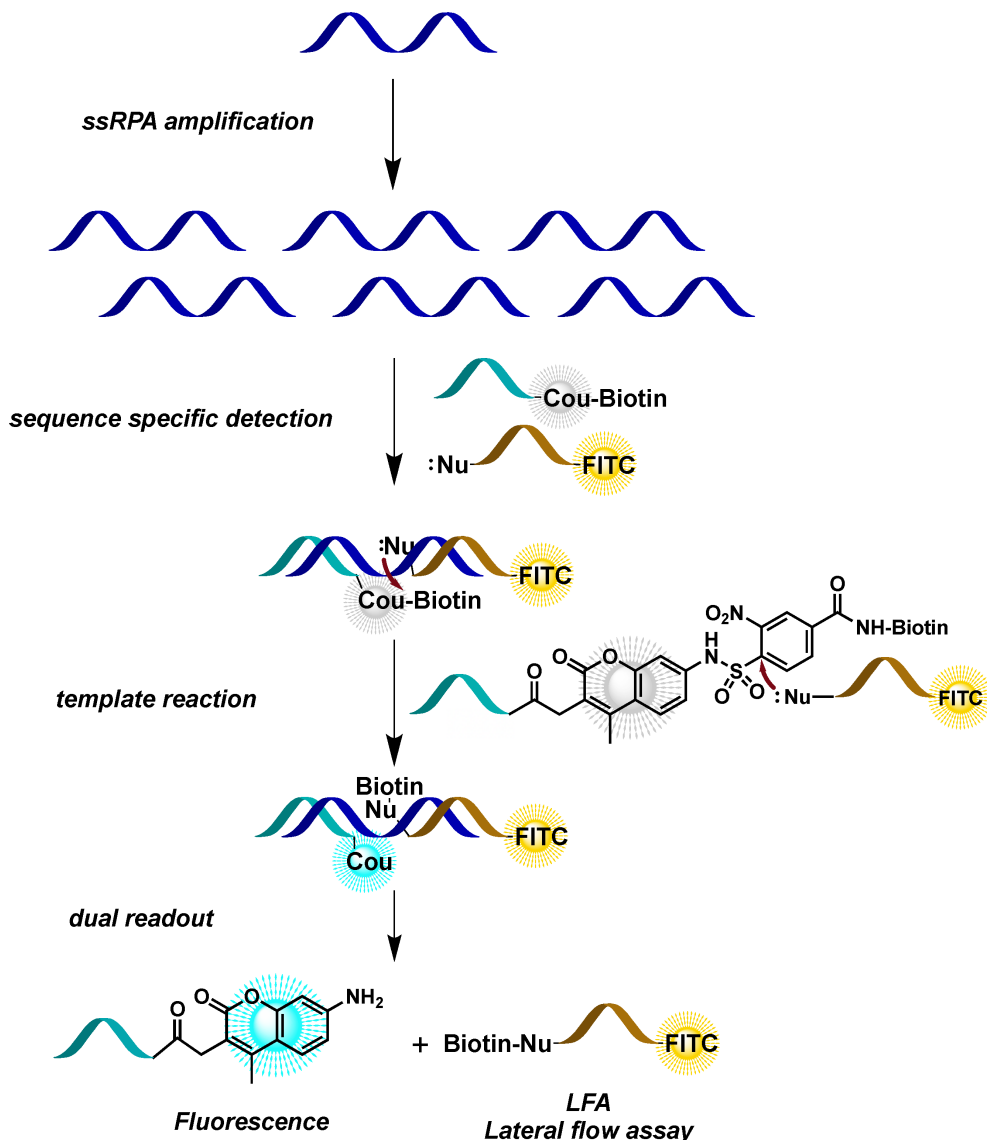


**FIGURE 1** Dual-readout DNA detection. DNA detection by *single-strand* RPA + templated reaction with fluorescence and LFA dual-readout

spacer followed by coupling of the desired nucleophile (either the 4-Methyltrityl (Mtt) protected 4-mercaptobenzoic acid or 4,4'-[Diselenobis(methylene)]bis[benzoic acid]).

For the synthesis of the PNA probes containing fluorescein and nucleophile (HX-PNA-FITC), the same procedure was followed with the exception that the Mtt protecting group on the last PNA monomer was kept. After having coupled the nucleophile, the Mtt on the PNA was deprotected, and an Fmoc-Lys(Mtt)-OH was coupled at the N' terminus. Finally, the Fmoc of the lysine was deprotected followed by acetylation of the free amine, and the Mtt was also deprotected followed by an FITC coupling. Fluorescein isothiocyanate (FITC) was coupled on the side chain of a lysine to avoid Edman degradation.

For the PNA probes containing Coumarin-Biotin (Cou-Biotin) (PNA-Cou-Biotin), the synthesis of the 8 $nb$  PNA was followed by the coupling of an Fmoc-Lys(N<sub>3</sub>)-OH at the N' terminus of the

sequence. After Fmoc deprotection and acetylation of the free amine, the PNA sequence was cleaved and deprotected. The PNA probe carrying an azide was then reacted with the Cou-Biotin (S9) compound bearing an alkyne through a copper(I)-catalyzed azide-alkyne cycloaddition (CuAAC). Briefly, to a mixture of 1.4 mL of water and 200  $\mu$ L of DMSO were added 160  $\mu$ L of CuSO<sub>4</sub> 45 mM (7.2 mmol, 12.5 equiv.), 160  $\mu$ L of tris[[1-hydroxy-propyl-1H-1,2,3-triazol-4-yl]methyl]amine (THPTA) 90 mM (14.4 mmol, 25 equiv.), 160  $\mu$ L of sodium Ascorbate (NaAsc) 90 mM (14.4 mmol, 25 equiv.), 100  $\mu$ L of the alkyne component at 20 mM (1.7 mmol, 3 equiv.) and 100  $\mu$ L of the azide partner at 5 mM (0.6 mmol, 1 equiv.). The reaction was stirred for 2 h at room temperature, and the desired product was purified by HPLC.

The PNA probes used in the templated reactions (written from C' to N') with their expected and measured mass (m/z, either by LC-MS

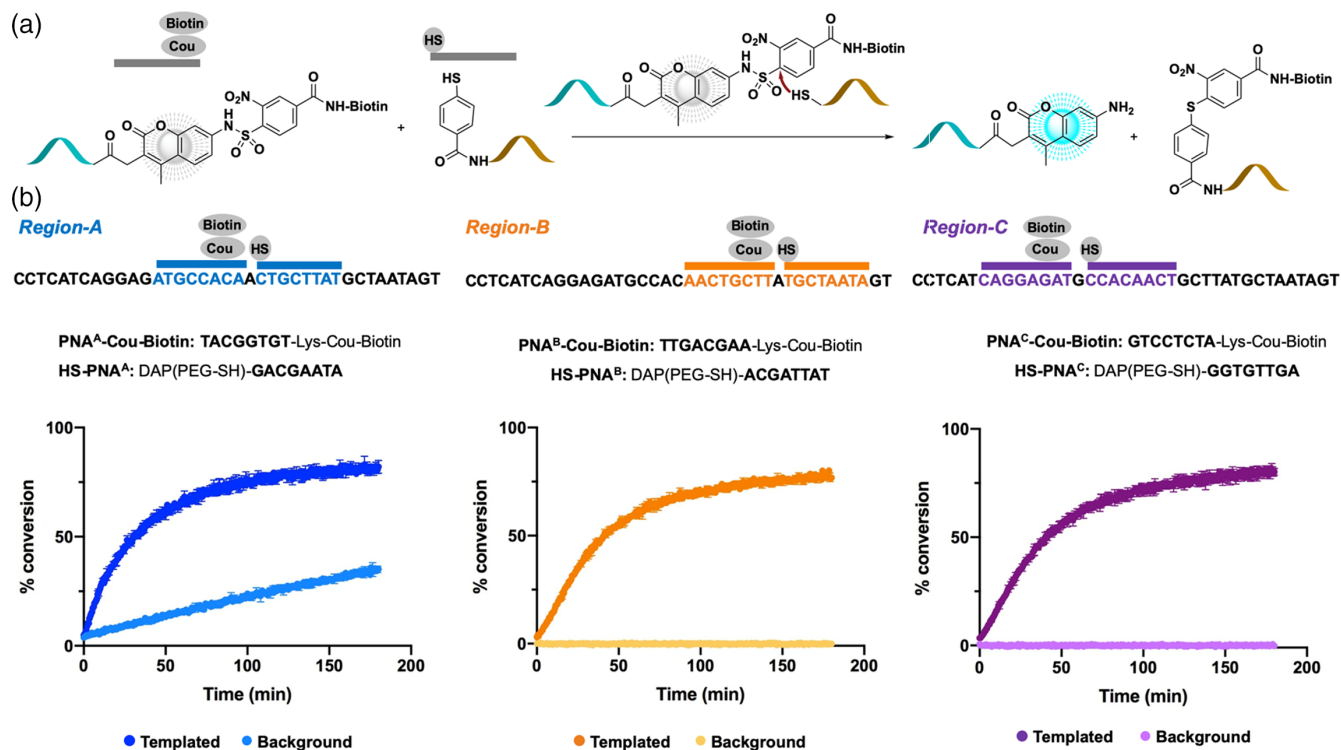


**FIGURE 2** Templated reaction optimization. (a)  $S_NAr$  reaction mechanism between  $PNA^X$ -Cou-Biotin and  $HS-PNA^X$ . (b) DNA template region, PNA probes and kinetics of templated reaction for the three different designs (a-c) targeting three different regions of the DNA template. The two different probes for each design are shown with the PNA sequence in bold. Kinetics of the templated reaction are shown in dark color for templated reaction (200 nM  $PNA^X$ -Cou-Biotin + 400 nM  $HS-PNA^X$  + 300 nM 38<sub>nb</sub> DNA) and light color for background reaction (200 nM  $PNA^X$ -Cou-Biotin + 400 nM  $HS-PNA^X$ ). Each data point is the mean value of three replicates represented as a dot with the corresponding SD as an error bar

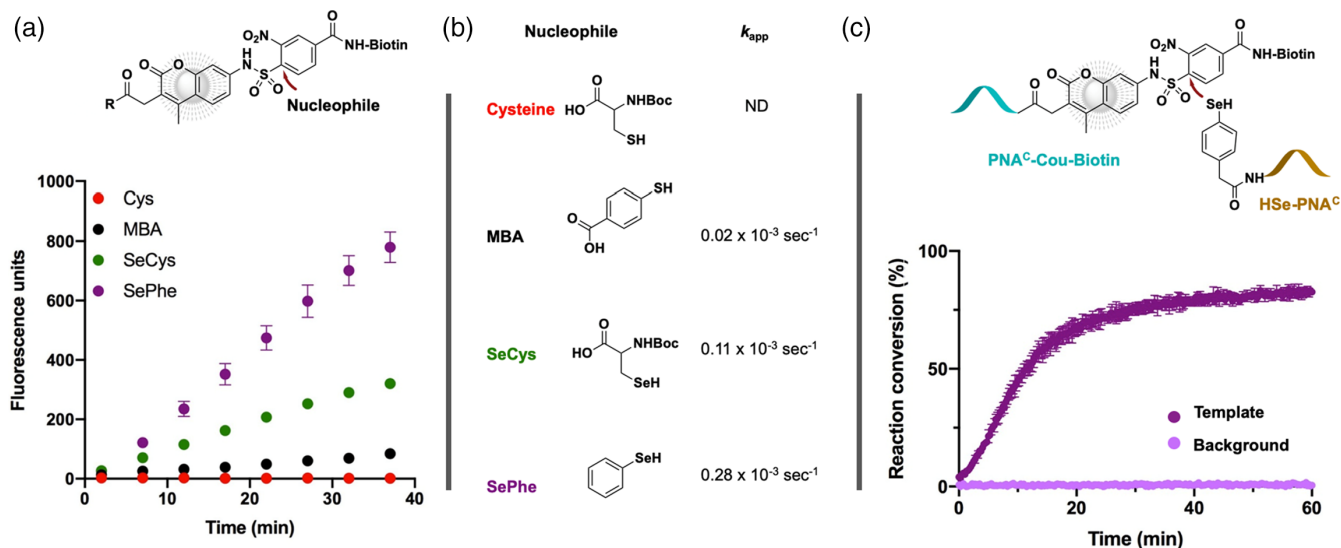


**FIGURE 3** Accelerating the templated reaction. (a) Pseudo-first order kinetics analysis of the bimolecular reaction using different nucleophiles. Reaction fluorescence intensities measured over time using as a nucleophile N-Boc-cysteine in red, 4-mercaptobenzoic acid (MBA) in black, N-Boc selenocysteine in green or selenophenol (SePhe) in purple (1  $\mu\text{M}$   $PNA^C$ -Cou-Biotin and 500  $\mu\text{M}$  of the corresponding nucleophile in PBSt + 2 mM TCEP). The reactions were monitored by excitation at 355 nm and emission at 450 nm. The data were analyzed by linear regression as a pseudo first-order kinetics ( $(\ln[AMCA])/t$ ). (b) Pseudo first-order rate constants of  $PNA^C$ -Cou-Biotin with different nucleophiles measured in panel A. (c) DNA-templated reaction with HSe- $PNA^C$  probe. Reaction conversion of the templated reaction with 400 nM of HSe- $PNA^C$  probe, 200 nM  $PNA^C$ -Cou-Biotin, 300 nM template DNA, 2 mM TCEP in PBSt buffer. Each data point is the mean value of three replicates, represented as a dot with the corresponding SD as an error bar

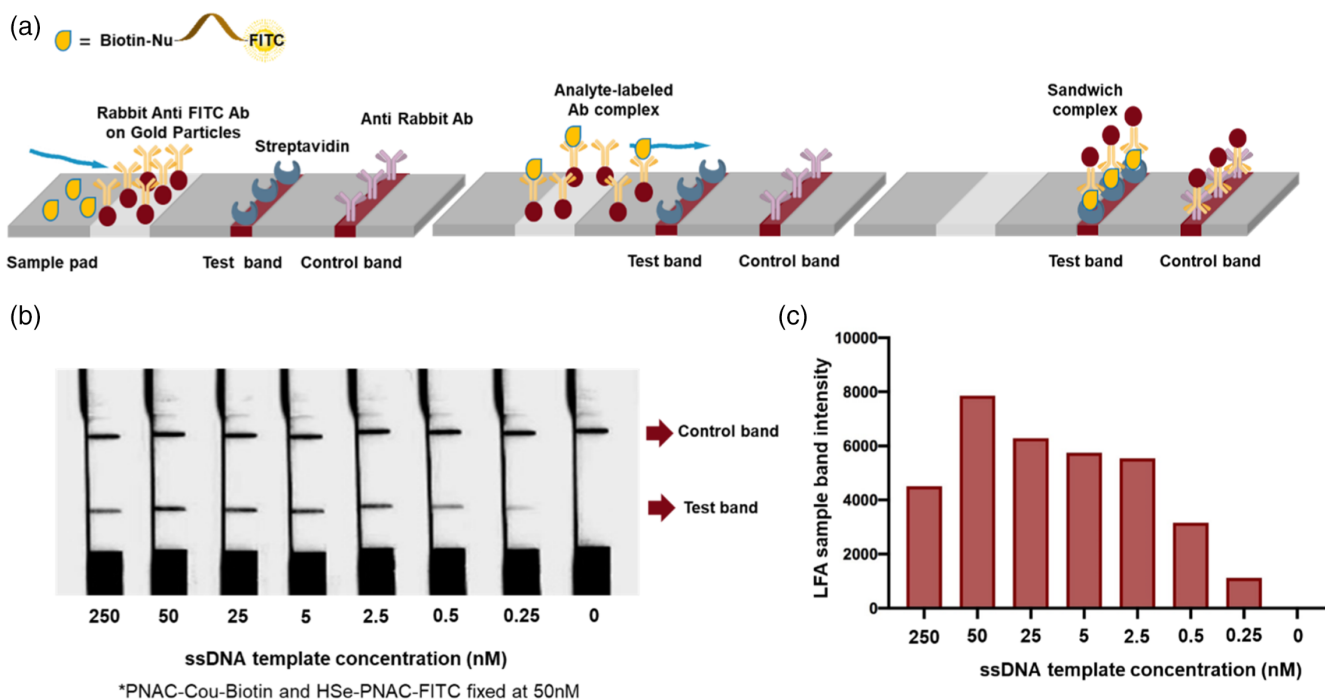


**FIGURE 4** DNA-templated reaction with different equivalents of template. (a) Graphical scheme of the lateral flow assay (LFA). (b) Lateral flow assay (LFA) of the templated reaction with different concentrations of DNA template. PNA<sup>C</sup>-Cou-Biotin and HSe-PNA<sup>C</sup>-FITC both at 50 nM and different concentrations of template DNA, in PBSt +2 mM TCEP for 90 min. (c) Signal quantification of the test band in the different LFAs in panel B

or MALDI) are: PNA<sup>A</sup>-Cou-Biotin (T\*AC\*GG\*TG\*T-Lys(Cou-Biotin)-Ac) Expected: 3314.2 Found: 3314.3, HS-PNA<sup>A</sup> (DAP[PEG-SH]-GA\*CG\*AA\*TA\*-Ac) Expected: 2748.1 Found: 2748.4, PNA<sup>B</sup>-Cou-Biotin (T\*TG\*AC\*GA\*A-Lys(Cou-Biotin)-Ac) Expected: 3307.2 Found: 3307.0, HS-PNA<sup>B</sup> (DAP[PEG-SH]-AC\*GA\*TT\*AT\*-Ac) Expected: 2714.1 Found: 2713.9, PNA<sup>C</sup>-Cou-Biotin (G\*TC\*CT\*CT\*A-Lys(Cou-Biotin)-Ac) Expected: 3234.2 Found: 3234.0, HS-PNA<sup>C</sup> (DAP[PEG-SH]-GG\*TG\*TT\*GA\*-Ac) Expected: 2786.1 Found: 2785.7, HSe-PNA<sup>C</sup> (DAP[PEG-SeH]-GG\*TG\*TT\*GA\*-Ac) Expected: 2806.0 Found: 2806.1, HSe-PNA<sup>C</sup>-FITC (DAP[PEG-SeH]-GG\*TG\*TT\*GA\*-Lys(FITC)-Ac) Expected: 3407.2 Found: 3407.0.

## 2.2 | DNA templated reaction optimization

Templated reactions were carried out in a 96 well plate in a final volume of 200  $\mu$ L at pH 7.4. The reactions were performed by sequentially adding 8  $\mu$ L of 50 mM tris(2-carboxyethyl)phosphine (TCEP), Nu-PNA, 38nb DNA template, and PNA-Cou-Biotin at the desired concentrations. The reactions were performed at 37  $^{\circ}$ C, and the fluorescence intensity was monitored with a plate reader with the following conditions: excitation, 355 nm, emission, 450 nm. The conversion within a given templated reaction was calculated by comparing the fluorescence level to the starting fluorescence values and the maximum fluorescence intensity achieved after adding an excess of Nu-PNA, DNA template, and TCEP (to push the templated reaction to 100% conversion). S<sub>N</sub>Ar reaction of PNA-Cou-Biotin with excess nucleophile was shown to proceed to completion by

LC-MS analysis (Supplementary information 6). A shorter version of the 135nb DNA (used for RPA amplification) which does not contain the primer regions (38nb DNA template - 5'-CCTCATCAGGATGCCAC AACTGCTTATGCTAATAGT-3'), was used as the template in reaction optimization.

## 2.3 | RPA + Lambda exonuclease degradation

Following the general procedure of the RPA TwistAmp Basic kit (TwistDx: TABAS03KIT), RPA was carried out in a PCR tube in a final volume of 51.5  $\mu$ L and 500 nM of primers. The amplification was initiated as follows: 29.5  $\mu$ L of primer-free rehydration buffer were mixed with 5  $\mu$ L of water, 5  $\mu$ L of 10  $\mu$ M Cy3 labeled forward primer (5'-Cy3-GTGGCGGTTCACTATATGTTAAACCAGGTGGAA-3') and 5.0  $\mu$ L of 10  $\mu$ M phosphorylated reverse primer (5'-P-ATTGGCCGT GACAGCTTGACAAATGTTAAAAAC-3'). This solution was transferred to a TwistAmp Basic reaction kit followed by adding 1.0  $\mu$ L of analyte solution (DNA template at 2fM - 10<sup>3</sup> copies DNA/ $\mu$ L) and 5  $\mu$ L of Mg(OAc)<sub>2</sub> 280 mM. The reaction was incubated at 39  $^{\circ}$ C for 15 min and heated at 95  $^{\circ}$ C for 10 min. The RPA product was then centrifuged for 5 min at 14 k rpm, and the supernatant was mixed with 5.0  $\mu$ L of 10 $\times$  Lambda exonuclease buffer and 1.0  $\mu$ L of Lambda exonuclease (Bioconcept, M0262S). The reaction was incubated at 37  $^{\circ}$ C for 40 min. For reactions shown in Figure 5, the formation of the desired DNA was followed by gel analysis with 18% Native PAGE. The DNA was visualized by SYBR Gold Nucleic acid staining.

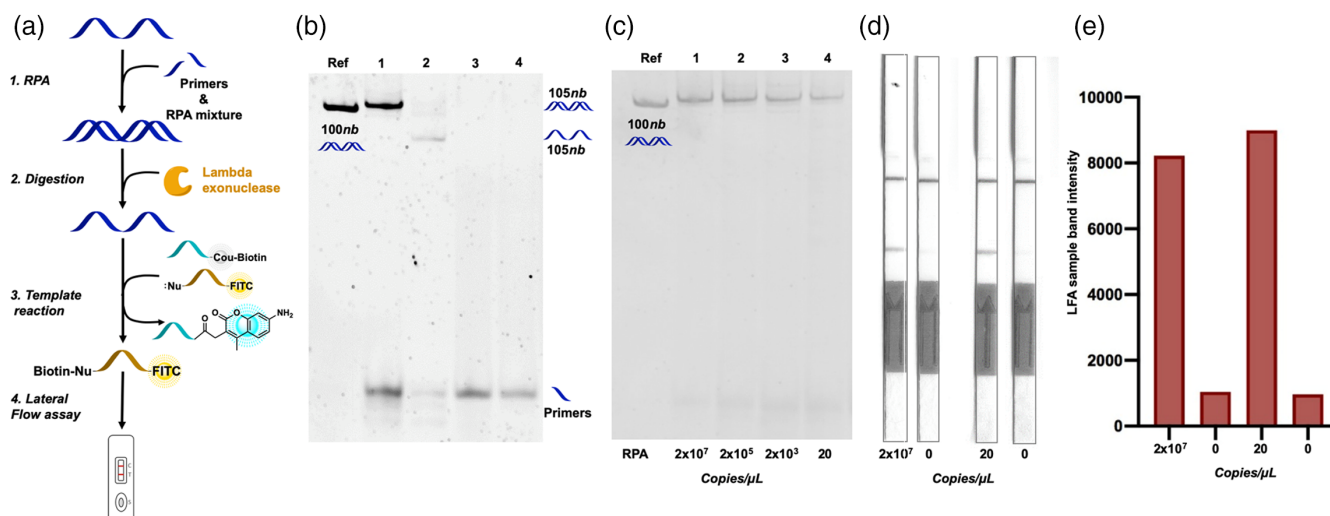


**FIGURE 5** DNA detection. (a) Protocol for DNA detection. (b) Following the *single-stranded* RPA with a Native-PAGE. 100 bp Ladder (Lane Ref), RPA amplification with the DNA template (Lane 1), RPA amplification with DNA template + Lambda degradation (Lane 2), RPA amplification without DNA template (Lane 3), RPA amplification without DNA template + Lambda degradation (Lane 4). DNA on the Native-PAGE was stained with SYBR gold. C) RPA amplification with serial dilution of DNA. 100 bp Ladder (Lane Ref), RPA with  $2 \times 10^7$  copies/ $\mu\text{L}$  of DNA template (Lane 1), RPA with  $2 \times 10^5$  copies/ $\mu\text{L}$  of DNA template (Lane 2), RPA with  $2 \times 10^3$  copies/ $\mu\text{L}$  of DNA template (Lane 3), RPA with 20 copies/ $\mu\text{L}$  of DNA template (Lane 4). DNA on the Native-PAGE was stained with SYBR gold. D) SARS-CoV-2 DNA detection by “*single-stranded* RPA + Templated reaction + LFA” with and without 20 copies/ $\mu\text{L}$  of DNA template. E) Quantification of the sample band on the LFA in panel D

The 135nb DNA template used for RPA amplification corresponds to the nucleotides 15 418-15 554 of the SARS-CoV-2 genome (135nb DNA template, 5'-GCTCAAGTATTGAGTGAAATGGTCATGTG TGGCGGTTCACTATATGTTAAACCAGGTGGAA CCTCATCAG GAGATGCCACAACCTGCTTATGCTAATAGTGTTTTAAACATTTGTCA-AGCTGTACACGGCCAATGTT-3'). The designed primer set amplifies the following 105nb DNA sequence (5'-GTGGCGGTTCACTATATGT TAAACCAGGTGGAACCTCATCAGGAGATGCCACAACCTGCTTATGC-TAATAGTGTTTTAAACATTTGTCAAGCTGTACACGGCCAATG-3'). All DNA sequences were purchased from Eurogentec. For RT-RPA, the same procedure was used starting with a RNA analyte (Wuhan coronavirus 2019 RdRP gene control obtained from Charité/EVAg) with 1  $\mu\text{L}$  of RevertAid Reverse Transcriptase (Thermo Fisher Scientific, Ref:EPO441), 1  $\mu\text{L}$  of Recombinant RNasin Ribonuclease Inhibitor (Promega, Ref: N251A) and 1  $\mu\text{L}$  of PCR Nucleotide Mix (Promega, Ref:C114G) and the RT-RPA reaction was carried out for a total of 30 min.

## 2.4 | Detection of amplified DNA sequence

The ssDNA obtained after lambda exonuclease dsDNA degradation (40  $\mu\text{L}$ ) was diluted with 155  $\mu\text{L}$  of PBSt together with 8  $\mu\text{L}$  of TCEP 50 mM, 2  $\mu\text{L}$  of PNA<sup>C</sup>-Cou-Biotin (5  $\mu\text{M}$ ) and 2  $\mu\text{L}$  of HSe-PNA<sup>C</sup>-FITC (5  $\mu\text{M}$ ). The reaction was incubated for 40 min at room temperature, and 20  $\mu\text{L}$  of reaction were diluted into 80  $\mu\text{L}$  of LFA buffer before adding the LFA strip (Milenia GenLine HybriDetect Ref:MGHD 1).

## 3 | RESULTS AND DISCUSSION

Based on the initial indications by the WHO,<sup>[59]</sup> the 135nb DNA sequence corresponding to nucleotides 15 418-15 554 of the SARS-CoV-2 genome (NCBI Reference sequence: MN908947.3) was selected for amplification. Two primers of 33 nucleotides were used to amplify the DNA sequence, leaving a 38nb gap between the primer sites suitable for templated reaction with the amplicon. The choice of the length of the two PNA probes for templated reaction is crucial since there is a tradeoff between sensitivity (detection threshold) and specificity (single nucleotide discrimination) as well as turnover. Longer probes afford stable hybridization complex at lower concentration, but the penalty of a single mismatch is less severe and the turnover of probes on the template is slower. Based on our previous work showing a similar kinetics for the templated reaction between two 7nb and two 9nb PNAs at low nM concentration,<sup>[60,61]</sup> an 8nb PNA was chosen for the DNA templated reaction.

As shown in Figure 2, we designed probes targeting three different regions of the template, mindful that the reaction kinetics can be affected by unforeseen folding or cross-hybridization. The reactions proceeded with a strong increase in fluorescence as previously reported and consistent with the change of electronic donation of the amino group of the coumarin following S<sub>N</sub>Ar (Figure 2A).<sup>[49,62]</sup> While the probes corresponding to *region A* gave high background in the absence of the DNA template, probes corresponding to *regions B* and *C* afforded clean templated reaction without measurable background reaction at 200 nM concentration (Figure 2B). Templated reaction with the probes from *region C* showed a  $t_{1/2}$  of 42 min ( $k_{\text{app}} 0.28 \times 10^{-3} \text{ s}^{-1}$ ,

assuming a pseudo-first-order reaction) and was selected for further experiments.

Abe and co-worker had clearly shown that the substitution on the aryl sulfonamide had a strong impact on the kinetics of the reaction with a 2,4-dinitrosulfonamide reacting five times faster than 2-cyano-4-nitrosulfonamide.<sup>[49]</sup> Based on the substitution pattern of the aryl sulfonamide used in the present study, we anticipated and observed a slower reaction than had been reported by Abe *et al.* However, we reasoned that some reactivity could be regained by using selenol nucleophiles.<sup>[55]</sup> Changing from a thiol to a selenol not only benefit from a higher HOMO but also from higher acidity, which means a higher proportion of the nucleophile in the deprotonated state at neutral pH. To test this benefit, the pseudo-first-order rate constant between the PNA<sup>C</sup>-Cou-Biotin probe and four nucleophiles (Boc-cysteine, 4-mercaptobenzoic acid, Boc-selenocysteine, and selenophenol) was determined (Figure 3). While Boc-cysteine showed no measurable reaction under the reaction condition, Boc-selenocysteine reacted with a pseudo-first-order rate constant of  $0.11 \times 10^{-3} \text{ s}^{-1}$ , five times faster than 4-mercaptobenzoic acid. The fastest reaction was observed with selenophenol ( $0.28 \times 10^{-3} \text{ s}^{-1}$ ) reacting over ten times faster than 4-mercaptobenzoic acid (Figure 3a, b). Based on these results, a PNA probe was prepared with selenophenol (HSe-PNA<sup>C</sup>) and tested in templated reaction. Gratifyingly, the probe afforded a 4-fold rate acceleration in the templated reaction ( $t_{1/2}$  of 11 min and  $k_{\text{app}} 1.05 \times 10^{-3} \text{ s}^{-1}$ , assuming a pseudo-first order reaction) (Figure 3c) compared to the corresponding thiophenol PNA (HS-PNA<sup>C</sup>).

We next turned our attention to the detection by LFA using commercially available strips with a biotin capture band and gold nanoparticle-labeled-anti-fluorescein antibody (Figure 4A). The fluorescence and LFA readouts afforded a good correlation of the DNA-templated ligation (Figure S2). After optimizing the DNA-templated reaction using fluorescence readout, we next focused on using LFA for POC diagnostic. We tested the response as a function of template loading and quantified the results with ImageJ.<sup>[63]</sup> As shown in Figure 4b, c, the templated reaction yields a detectable signal down to 0.005 equivalents of DNA template (250 pM) relative to PNA probes (50 nM). Templated reactions that do not ligate the two PNA fragments after reaction allow for signal amplification, when PNA lengths are short enough to allow dynamic exchange on the template. As can be seen from the LFA detection, there is not a linear decrease in signal between 1 equivalent of template and 0.1 equivalent of template, suggesting that the output of the reaction has benefited from template turnover. Moreover, the reaction with 5 equivalents of template should give low yield if the probe hybridization is not dynamic since probes would be hybridized on the same template on only a fraction of the template, yet the output is ca. 50% of the output measure with 1 equivalent of template. These results confirm that the reaction affords a detectable signal in the window of concentration expected with an RPA amplification (500 nM of primers, 5-fold diluted for the templated reaction).

The results shown thus far were done using a ssDNA template, but the RPA affords double-strand amplicon, and the short PNA

probes are unlikely to invade the dsDNA amplicon with meaningful yield. Preliminary experiments adding the PNA probes directly to the RPA reaction did not yield encouraging results. We first explored *asymmetric* amplification using an excess of one of the two primers. However, *asymmetric* RPA led to an undesired amplification product that ran between the expected ssDNA and dsDNA in a native-polyacrylamide gel electrophoresis (native-PAGE) and was incompetent in the templated reaction. We explored the selective degradation of a single strand in the duplex. Lambda exonuclease had previously been used with RPA to convert dsDNA amplicon to ssDNA.<sup>[33]</sup> Lambda exonuclease degrades preferentially 5' phosphorylated DNA strands, and its activity is blocked by 5' modification, such as Cy3. Thus, RPA was performed with a 5'-Cy3-labeled forward primer which blocks degradation of the templated strand and 5'-PO<sub>4</sub> functionalized reverse primer (Figure 5a). As shown in Figure 5b, treatment of the crude RPA mixture (lane 1) with exonuclease led to the desired 105nb ssDNA with full conversion (lane 2). Control experiments performing the RPA without DNA template and subsequent digestion did not lead to any amplification (lanes 3–4). It is well established that RPA has the capacity to yield amplicon from few copies of template (1–30 copies).<sup>[29,31,32,34]</sup> We confirmed that in the assay conditions (RPA, 15 min), amplicon was observed and yielded a detectable positive band on the LFA strip at 20 copies of analyte/ $\mu\text{L}$  (Figure 5c–e). Moreover, this methodology allows the detection of viral RNA by adding reverse transcriptase into the RPA mixture (RT-RPA) (Figure S3).

## 4 | CONCLUSIONS

In summary, we have developed a nucleic acid-sensing system that combines the power of RPA amplification with the robustness and fidelity of DNA-templated reaction to provide a dual detection with real-time fluorescence monitoring or LFA for end-point measurement for end-user. The templated reaction uses an S<sub>N</sub>Ar, adapted from the work of Abe and coworkers, to achieve a transfer of biotin from one PNA strand to another, thus enabling the LFA detection with concomitant unmasking of the coumarin fluorescence. We showed that using selenophenol as the nucleophile in the S<sub>N</sub>Ar led to a dramatically faster reaction than thiophenol or even selenocysteine. Implementation of this nucleophile in the templated reaction affords a pseudo-first-order rate of  $1.05 \times 10^{-3} \text{ s}^{-1}$  with a reaction half-life of 11 min. To capitalize on the RPA, the dsDNA amplicon had to be converted to ssDNA template, which was efficiently achieved with an exonuclease, provided the RPA is performed with a 5'protected forward primer (such as Cy3 labeled) and 5'phosphorylated reverse primer. Combining the power of an RPA amplification with a DNA-templated reaction for the read-out enables the detection down to 20 copies of analyte/ $\mu\text{L}$  (2 zmol of analyte) of the diagnostic SARS-CoV-2 DNA sequence and should be applicable to other viruses. These developments contribute a new combination of amplification and detection that is amenable to next-generation POC diagnostics. A number of RPA-based formats have been reported for SARS-CoV-2 detection with RPA ranging from 15 to 30 min and detection

of the amplicon extending to 120 min (Table S1 for detailed time analysis and detection method).<sup>[29,31,33,34,36–39]</sup> A side-by-side comparison of the different techniques is challenging because each approach has unique advantages and limitations and the length of the RPA step are not identical leading to different levels of amplification. The present assay utilizes a 15 min RPA amplification followed by a 40 min exonuclease step and 40 min templated reaction step. The total assay time might be further compressed by optimizing the exonuclease step and combining this step with the templated chemistry. Moreover, the future development of microfluidic cartridges should enable a more streamlined process.

## ACKNOWLEDGMENTS

The work was funded by research funds from the University of Geneva and the département d'instruction public (DIP) du canton de Genève. Open access funding provided by Université de Genève.

## CONFLICT OF INTEREST

The authors declare no competing interests.

## DATA AVAILABILITY STATEMENT

The data supporting the findings of this study is available within this paper and its Supplementary Information. Raw data has been deposited on Zenodo (<https://doi.org/10.5281/zenodo.5512653>).

## ORCID

Nicolas Winssinger  <https://orcid.org/0000-0003-1636-7766>

## REFERENCES

- [1] A. Cassidy, A. Parle-McDermott, R. O'Kennedy, *Front. Mol. Biosci.* **2021**, *8*, 637559.
- [2] K. Mullis, F. Faloona, S. Scharf, R. Saiki, G. Horn, H. Erlich, *Cold Spring Harb. Symp.* **1986**, *51*, 263.
- [3] F. Watzinger, K. Ebner, T. Lion, *Molecul. Aspects Med.* **2006**, *27*, 254.
- [4] E. Navarro, G. Serrano-Heras, M. J. Castano, J. Solera, *Clin. Chim. Acta* **2015**, *439*, 231.
- [5] R. Higuchi, G. Dollinger, P. S. Walsh, R. Griffith, *Bio-Technol.* **1992**, *10*, 413.
- [6] R. S. Tuma, M. P. Beaudet, X. K. Jin, L. J. Jones, C. Y. Cheung, S. Yue, V. L. Singer, *Anal. Biochem.* **1999**, *268*, 278.
- [7] V. V. Didenko, *BioTechniques* **2001**, *31*, 1106.
- [8] L. E. Morrison, T. C. Halder, L. M. Stols, *Anal. Biochem.* **1989**, *183*, 231.
- [9] A. McDermott, *Pr. Natl. Acad. Sci. USA* **2020**, *117*, 25956.
- [10] O. Vandenberg, D. Martiny, O. Rochas, A. van Belkum, Z. Kozlakidis, *Nat. Rev. Microbiol.* **2021**, *19*, 171.
- [11] T. Peto, U. C.-L. F. Oversight, *Eclinicalmedicine* **2021**, *36*, 100924.
- [12] L. J. Krüger, M. Gaedert, L. Köppel, L. E. Brümmer, C. Gottschalk, I. B. Miranda, P. Schnitzler, H. G. Kräusslich, A. K. Lindner, O. Nikolai, F. P. Mockenhaupt, J. Seybold, V. M. Corman, C. Drosten, N. R. Pollock, A. I. Cubas-Atienzar, K. Kontogianni, A. Collins, A. H. Wright, B. Knorr, A. Welker, M. De Vos, J. A. Sacks, E. R. Adams, C. M. Denkinger, *Cold Spring Harbor Laboratory, CSHL Press, Long Island, New York* **2020**.
- [13] T. Notomi, Y. Mori, N. Tomita, H. Kanda, *J. Microbiol.* **2015**, *53*, 1.
- [14] X. Z. Zhang, S. B. Lowe, J. J. Gooding, *Biosens. Bioelectron.* **2014**, *61*, 491.
- [15] B.-T. Teoh, S.-S. Sam, K.-K. Tan, J. Johari, M. B. Danlami, P.-S. Hooi, R. Md-Esa, S. Abubakar, *BMC Infect. Disea.* **2013**, *13*, 387.
- [16] O. Piepenburg, C. H. Williams, D. L. Stemple, N. A. Armes, *PLoS Biol.* **2006**, *4*, 1115.
- [17] Y. Yang, X. D. Qin, G. X. Wang, Y. Zhang, Y. J. Shang, Z. D. Zhang, *Virolog. J.* **2015**, *12*.
- [18] M. L. Powell, F. R. Bowler, A. J. Martinez, C. J. Greenwood, N. Armes, O. Piepenburg, *Anal. Biochem.* **2018**, *543*, 108.
- [19] P. Subsoontorn, M. Lohitnavy, C. Kongkaew, *Sci. Rep.* **2020**, *10*, 22349.
- [20] A. Ganguli, A. Mostafa, J. Berger, M. Y. Aydin, F. Sun, S. A. S. de Ramirez, E. Valera, B. T. Cunningham, W. P. King, R. Bashir, *Pr. Natl. Acad. Sci. USA* **2020**, *117*, 22727.
- [21] B. Schermer, F. Fabretti, M. Damagnez, V. Di Cristanziano, E. Heger, S. Arjune, N. A. Tanner, T. Imhof, M. Koch, A. Ladha, J. Joung, J. S. Gootenberg, O. O. Abudayyeh, V. Burst, F. Zhang, F. Klein, T. Benzing, R. U. Muller, *PLoS One* **2020**, *15*, e0238612.
- [22] V. L. D. Thi, K. Herbst, K. Boerner, M. Meurer, L. P. M. Kremer, D. Kirrmaier, A. Freistaedter, D. Papagiannidis, C. Galmozzi, M. L. Stanifer, S. Boulant, S. Klein, P. Chlanda, D. Khalid, I. B. Miranda, P. Schnitzler, H. G. Krausslich, M. Knop, S. Anders, *Sci. Translat. Med.* **2020**, *12*, eabc7075.
- [23] R. Lu, X. Wu, Z. Wan, Y. Li, X. Jin, C. Zhang, *Int. J. Mol. Sci.* **2020**, *21*, 2826.
- [24] L. Yu, S. Wu, X. Hao, X. Dong, L. Mao, V. Pelechano, W.-H. Chen, X. Yin, *Clin. Chem.* **2020**, *66*, 975.
- [25] G.-S. Park, K. Ku, S.-H. Baek, S.-J. Kim, S. I. Kim, B.-T. Kim, J.-S. J. Maeng, *Mol. Diagno.* **2020**, *22*, 729.
- [26] L. E. Lamb, S. N. Bartolone, E. Ward, M. B. Chancellor, *PLoS One* **2020**, *15*, e0234682.
- [27] C. Yan, J. Cui, L. Huang, B. Du, L. Chen, G. Xue, S. Li, W. Zhang, L. Zhao, Y. Sun, H. Yao, N. Li, H. Zhao, Y. Feng, S. Liu, Q. Zhang, D. Liu, J. Yuan, *Clin. Microbiol. Infec.* **2020**, *26*, 773.
- [28] Y. H. Baek, J. Um, K. J. C. Antigua, J.-H. Park, Y. Kim, S. Oh, Y.-I. Kim, W.-S. Choi, S. G. Kim, J. H. Jeong, B. S. Chin, H. D. G. Nicolas, J.-Y. Ahn, K. S. Shin, Y. K. Choi, J.-S. Park, M.-S. Song, *Emerg. Microbes Infect* **2020**, *9*, 998.
- [29] Y. Kim, A. B. Yaseen, J. Y. Kishi, F. Hong, S. K. Saka, K. Sheng, N. Gopalkrishnan, T. E. Schaus, P. Yin, *Cold Spring Harbor Laboratory, CSHL Press, Long Island, New York* **2020**.
- [30] O. Behrmann, I. Bachmann, M. Spiegel, M. Schramm, A. Abd El Wahed, G. Dobler, G. Dame, F. T. Hufert, *Clin. Chem.* **2020**, *66*, 1047.
- [31] J. Qian, S. A. Boswell, C. Chidley, Z.-X. Lu, M. E. Pettit, B. L. Gaudio, J. M. Fajnzylber, R. T. Ingram, R. H. Ward, J. Z. Li, M. Springer, *Nat. Commun.* **2020**, *11*, 5920.
- [32] S. M. Xia, X. Chen, *Cell Discovery* **2020**, *6*, 37.
- [33] M. H. Choi, J. Lee, Y. J. Seo, *Theor. Chim. Acta* **2021**, *1158*, 338390.
- [34] D. Liu, H. C. Shen, Y. Q. Zhang, D. Y. Shen, M. Y. Zhu, Y. L. Song, Z. Zhu, C. Y. Yang, *Lab Chip* **2021**, *21*, 2019.
- [35] J. P. Broughton, X. D. Deng, G. X. Yu, C. L. Fasching, V. Servellita, J. Singh, X. Miao, J. A. Streithorst, A. Granados, A. Sotomayor-Gonzalez, K. Zorn, A. Gopez, E. Hsu, W. Gu, S. Miller, C. Y. Pan, H. Guevara, D. A. Wadford, J. S. Chen, C. Y. Chiu, *Nat. Biotechnol.* **2020**, *38*, 870.
- [36] X. Ding, K. Yin, Z. Y. Li, R. V. Lalla, E. Ballesteros, M. M. Sfeir, C. C. Liu, *Nat. Commun.* **2020**, *11*, 4711.
- [37] Y. Y. Sun, L. Yu, C. X. Liu, S. T. Ye, W. Chen, D. C. Li, W. R. Huang, *J. Transl. Med.* **2021**, *19*.
- [38] E. Xiong, L. Jiang, T. A. Tian, M. L. Hu, H. H. Yue, M. Q. Huang, W. Lin, Y. Z. Jiang, D. B. Zhu, X. M. Zhou, *Angew. Chem., Int. Ed.* **2021**, *60*, 5307.
- [39] K. F. Yang, J. C. Chaput, *J. Am. Chem. Soc.* **2021**, *143*, 8957.
- [40] Z. A. Crannell, B. Rohrman, R. Richards-Kortum, *PLoS One* **2014**, *9*, e112146.

- [41] A. P. Silverman, E. T. Kool, *Chem. Rev.* **2006**, *106*, 3775.
- [42] A. Shibata, H. Abe, Y. Ito, *Molecules* **2012**, *17*, 2446.
- [43] K. Gorska, N. Winssinger, *Angew. Chem., Int. Ed.* **2013**, *52*, 6820.
- [44] C. Percivalle, J. F. Bartolo, S. Ladame, *Org. Biomol. Chem.* **2013**, *11*, 16.
- [45] M. Di Pisa, O. Seitz, *ChemMedChem* **2017**, *12*, 872.
- [46] B. Giri, S. Pandey, R. Shrestha, K. Pokharel, F. S. Ligler, B. B. Neupane, *Anal. Bioanal. Chem.* **2021**, *413*, 35.
- [47] K. M. Koczula, A. Gallotta, *Biosensor Technologies for Detection of Biomolecules* **2016**, *60*, 111.
- [48] M. Sajid, A.-N. Kawde, M. J. Daud, *Saudi Chem. Soc.* **2015**, *19*, 689.
- [49] A. Shibata, T. Uzawa, Y. Nakashima, M. Ito, Y. Nakano, S. Shuto, Y. Ito, H. Abe, *J. Am. Chem. Soc.* **2013**, *135*, 14172.
- [50] M. Egholm, O. Buchardt, L. Christensen, C. Behrens, S. M. Freier, D. A. Driver, R. H. Berg, S. K. Kim, B. Norden, P. E. Nielsen, *Nature* **1993**, *365*, 566.
- [51] A. Dragulescu-Andrasi, S. Rapireddy, B. M. Frezza, C. Gayathri, R. R. Gil, D. H. Ly, *J. Am. Chem. Soc.* **2006**, *128*, 10258.
- [52] J. Saarbach, P. M. Sabale, N. Winssinger, *Curr. Opin. Chem. Biol.* **2019**, *52*, 112.
- [53] A. Roloff, O. Seitz, *Chem. Sci.* **2013**, *4*, 432.
- [54] K. T. Kim, N. Winssinger, *Chem. Sci.* **2020**, *11*, 4150.
- [55] J. Sayers, R. J. Payne, N. Winssinger, *Chem. Sci.* **2018**, *9*, 896.
- [56] S. Pavagada, R. B. Channon, J. Y. H. Chang, S. H. Kim, D. MacIntyre, P. R. Bennett, V. Terzidou, S. Ladame, *Chem. Commun.* **2019**, *55*, 12451.
- [57] D. Chouikhi, M. Ciobanu, C. Zambaldo, V. Duplan, S. Barluenga, N. Winssinger, *Chem. – Eur. J.* **2012**, *18*, 12698.
- [58] C. Zambaldo, S. Barluenga, N. Winssinger, *Curr. Opin. Chem. Biol.* **2015**, *26*, 8.
- [59] V. M. Corman, O. Landt, M. Kaiser, R. Molenkamp, A. Meijer, D. K. W. Chu, T. Bleicker, S. Brünink, J. Schneider, M. L. Schmidt, D. G. J. C. Mulders, B. L. Haagmans, B. van der Veer, S. van den Brink, L. Wijsman, G. Goderski, J.-L. Romette, J. Ellis, M. Zambon, M. Peiris, H. Goossens, C. Reusken, M. P. G. Koopmans, C. Drosten, *Euro. Surveill.* **2020**, *25*, 2000045.
- [60] D. Chang, E. Lindberg, N. Winssinger, *J. Am. Chem. Soc.* **2017**, *139*, 1444.
- [61] D. Chang, K. T. Kim, E. Lindberg, N. Winssinger, *Bioconjugate Chem.* **2018**, *29*, 158.
- [62] A. Shibata, H. Abe, M. Ito, Y. Kondo, S. Shimizu, K. Aikawa, Y. Ito, *Chem. Commun.* **2009**, 6586.
- [63] C. A. Schneider, W. S. Rasband, K. W. Eliceiri, *Nat. Methods* **2012**, *9*, 671.

#### SUPPORTING INFORMATION

Additional supporting information may be found in the online version of the article at the publisher's website.

**How to cite this article:** L. Farrera-Soler, A. Gonse, K. T. Kim, S. Barluenga, N. Winssinger, *Biopolymers* **2022**, *113*(4), e23485. <https://doi.org/10.1002/bip.23485>